

Supplementary information : Probing thermal expansion of graphene and modal dispersion at low-temperature using graphene NEMS resonators

Vibhor Singh¹, Shamashis Sengupta¹, Hari S. Solanki¹, Rohan Dhall¹, Adrien Allain¹, Sajal Dhara¹, Prita Pant² and Mandar M. Deshmukh¹

¹Department of Condensed Matter Physics, TIFR, Homi Bhabha Road, Mumbai 400005 India

²Department of Metallurgical Engineering and Materials Science, IIT Bombay Powai, Mumbai : 400076, India

E-mail: deshmukh@tifr.res.in

1. Raman spectroscopy of the suspended graphene devices

We performed Raman spectroscopy to confirm the number of layers in our suspended graphene devices. Figure 1 shows the 2D band from one of the devices with a single Lorentzian fit confirming it to be a monolayer graphene device.

2. Change of conductance with gate voltage for device D1

Figure 2 shows the change of conductance with gate voltage for device D1 at 7K. The position of Dirac point at 13V can be seen clearly.

3. Etching under the gold electrode

The gold electrodes support the graphene membrane and the silicon oxide under the graphene supported by gold electrodes is removed during the wet etch. To confirm this, we took a suspended graphene device, and mildly sonicated it to remove the graphene flake. Figure 3 shows a tilted scanning electron microscope image of such a 3 probe device. The dashed outline shows the position of the suspended graphene flake before its removal by sonication. It can be seen from the image that during sonication, part of the gold electrodes covering the graphene flake before sonication has also been removed, revealing the etched SiO₂ under the electrode covering graphene flake. This clearly shows that HF etching removes the SiO₂ uniformly under the graphene flake. However, for metal electrodes that do not cover graphene a thin wall of SiO₂ supports the electrodes; this is also clearly seen in Figure 1a in the main text.

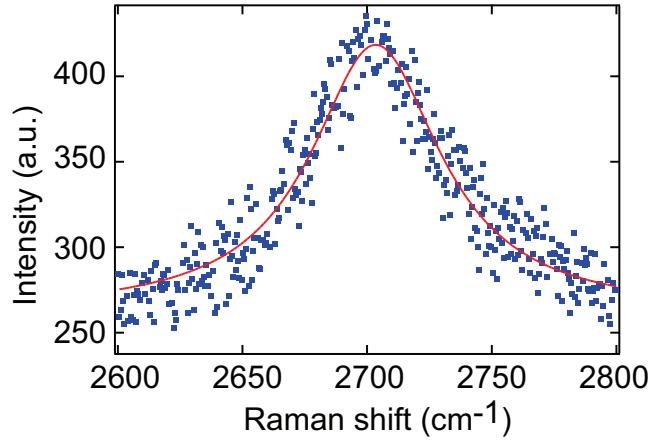


Figure 1. Raman data shows the spectrum of 2G band fitted with single Lorentzian.

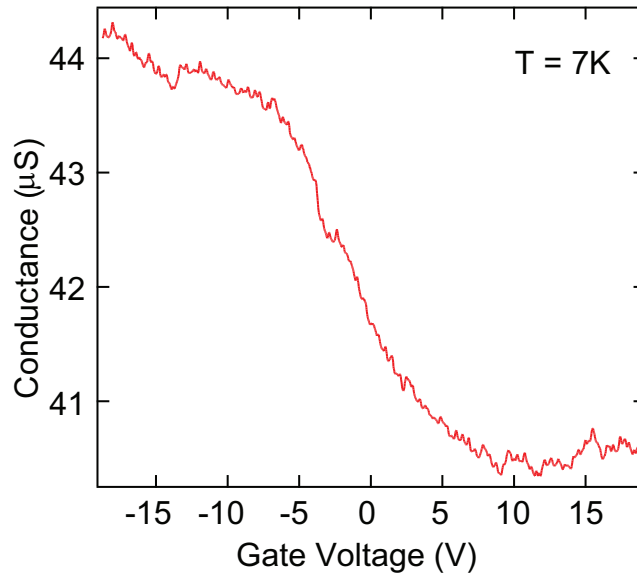


Figure 2. The change of conductance as a function of gate voltage.

4. Modeling the resonant frequency dispersion with gate voltage

A graphene sheet is held between two electrodes distance D apart. Distance measured along the length of the sheet from any one end is denoted by x and $z(x)$ is the distance by which it is pulled towards the substrate due to an applied gate voltage. Equation describing the vibration of a membrane is

$$\rho t \frac{\partial^2 z}{\partial \tau^2} = \frac{\Gamma}{w} \frac{\partial^2 z}{\partial x^2} + F(x), \quad (1)$$

where $F(x)$ is the externally applied force per unit area, Γ is the tension, ρ is the mass density of graphene, w is the width of the flake, t is the thickness and τ is the time.

The capacitive force per unit area at a point on the membrane is assumed to have the same form as that for an infinite parallel plate capacitor, depending on the height

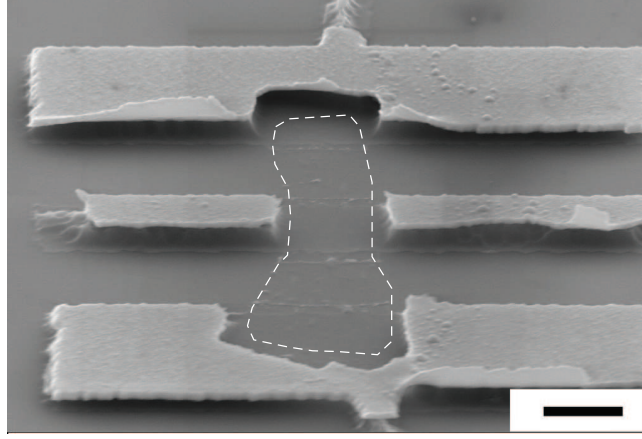


Figure 3. Tilted SEM image of a suspended graphene device after removal of the graphene flake. The dashed outline shows the original position of the graphene flake. The scale bar corresponds to 1 μm .

of the point above the substrate.

$$F(x) = \frac{\varepsilon_0 V^2}{2[R - z(x)]^2} \simeq \frac{\varepsilon_0}{2R^2} V^2 + \frac{\varepsilon_0}{R^3} V^2 z(x), \quad (2)$$

where R is the height above which the sheet is suspended and V is the potential difference between two plates of the capacitor. At an applied DC gate voltage V_g^{DC} , the bending of the sheet, assuming $z(x) \ll R$ can be expressed as

$$z(x) = \frac{\varepsilon_0 w V_g^{DC2}}{4R^2 \Gamma} (Dx - x^2). \quad (3)$$

We denote the distance between the electrodes as D . The actual length of the stretched graphene sheet is

$$\int_0^D \sqrt{1 + \left(\frac{\partial z}{\partial x}\right)^2} dx \simeq D + \frac{\varepsilon_0^2 w^2 D^3 (V_g^{DC})^4}{96 \Gamma^2 R^4}. \quad (4)$$

Let us denote by L_0 the length the sheet would have taken if tension was zero. From the stress-strain relationship, we can write

$$\frac{\Gamma}{wt} = \frac{E_{\text{graphene}}}{L_0} \left[D + \frac{\varepsilon_0^2 w^2 D^3 (V_g^{DC})^4}{96 \Gamma^2 R^4} - L_0 \right]. \quad (5)$$

The cubic equation in tension, written above, can be solved for the tension to get

$$\Gamma = \frac{\Gamma_0}{3} + \frac{\sqrt[3]{2}\Gamma_0^2}{3b} + \frac{b}{3\sqrt[3]{2}} \quad (6)$$

where, $b = \sqrt[3]{3\sqrt{3}\sqrt{27a^2 + 4a\Gamma_0^3} + 27a + 2\Gamma_0^3}$, $a = \frac{\varepsilon_0^2 w^2 D^3 (V_g^{DC})^4}{96 \Gamma^2 R^4}$ and $\Gamma_0 = E_{\text{graphene}} wt \left(\frac{D - L_0}{L_0} \right)$.

From Equation 1, we can write down the equation for the small oscillation of the membrane about the equilibrium configuration

$$\rho t \frac{\partial^2 \delta z}{\partial \tau^2} = \frac{\Gamma}{w} \frac{\partial^2 \delta z}{\partial x^2} + \frac{\varepsilon_0 (V_g^{DC})^2}{R^3} \delta z, \quad (7)$$

where the small displacement δz is a function of both x and time τ . The fundamental resonant frequency is given by

$$f_0 = \frac{1}{2\pi} \sqrt{\frac{\pi^2 \Gamma}{D^2 \rho t w} - \frac{\varepsilon_0 (V_g^{DC})^2}{\rho t R^3}} \quad (8)$$

where Γ is given by Equation 6.

In order to gain more insight into Equation 8, we perform a Taylor series expansion of the Equation 6, which gives

$$\Gamma = E_{\text{graphene}} w t \left(\frac{D - L_0}{L_0} \right) + \frac{\varepsilon_0^2 D^3 w L_0}{96 E_{\text{graphene}} t R^4 (D - L_0)^2} (V_g^{DC})^4 + H.O. \quad (9)$$

This leads to

$$f_0 \simeq \frac{1}{2\pi} \sqrt{\frac{\pi^2 E_{\text{graphene}} (D - L_0)}{D^2 \rho L_0} - \frac{\varepsilon_0 (V_g^{DC})^2}{\rho t R^3} + \frac{\pi^2 \varepsilon_0^2 D L_0}{96 \rho E_{\text{graphene}} t^2 R^4 (D - L_0)^2} (V_g^{DC})^4} \quad (10)$$

5. Change of resonant frequency of the graphene resonator with temperature

At room temperature, most of the devices show positive dispersion with gate voltage (show an increase in the resonant frequency with $|V_g^{DC}|$). In all the devices, resonant frequency increases upon cooling and its tunability on gate voltage reduces. Figure 4 shows the resonant frequency dispersion with gate voltage at various temperatures for one of our devices (D3). Also, at low temperatures, in the vicinity of the zero gate voltage, we see negative dispersion (resonant frequency decreases with the increase in $|V_g^{DC}|$). Qualitatively, this behavior can be understood from Equation 10. The first term inside the square-root on the r.h.s of the Equation 10 comes from the in-built tension. As the temperature is lowered, $(D - L_0)$ increases since contraction of gold electrodes outweighs the thermal expansion of graphene and resonant frequency at $V_g^{DC} = 0$ goes up. Also, the coefficient of the $(V_g^{DC})^4$ inside the square root of Equation 10 decreases and fails to suppress the negative $(V_g^{DC})^2$ term, resulting in a prominent negative dispersion at low temperatures.

By using the Equation 8, we extract the mass density (ρ) and in-built tension (Γ_0) at any temperature. As we cool down the resonator, an independent measurement of ρ and Γ_0 becomes difficult as the tunability with gate voltage reduces. However, by assuming that mass density does not change upon cooling, we can estimate the in-built tension in resonator from the frequency at zero gate voltage, in that case Equation 8 just reduces to,

$$f_0(0) = \frac{1}{2L} \sqrt{\frac{\Gamma_0}{\rho w t}}. \quad (11)$$

At room temperature, Equation 8 describes the resonance frequency dispersion with V_g^{DC} accurately. However, Equation 8 fails to describe the resonant frequency dispersion with V_g^{DC} at lower temperatures quantitatively. To describe it quantitatively as well,

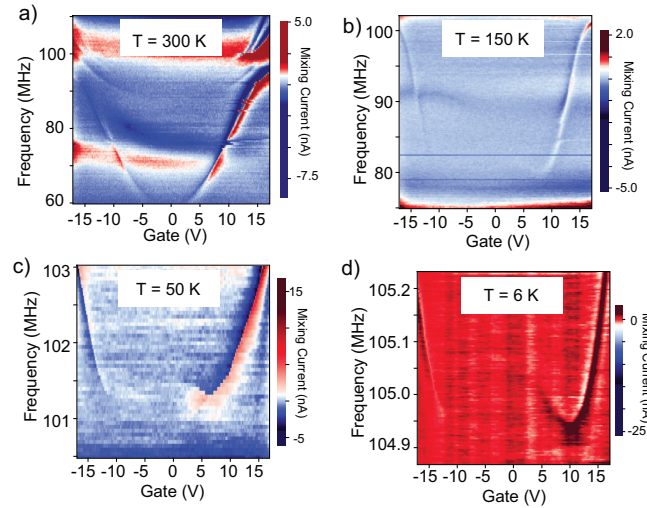


Figure 4. (a), (b), (c), (d) show the resonant frequency dispersion with gate voltage at 300K, 150K, 50K and 6K respectively.

we introduce one parameter λ while estimating the tension (see Equation 5) in the flake, $\Gamma = \lambda E_{\text{graphene}} w t \left(\frac{L-L_0}{L_0} \right)$. At room temperature $\lambda = 1$, however to fit the dispersion data at 6 K, $\lambda = 0.05$ is the optimum value. There can be many microscopic contributions towards this parameter that are not appropriately accounted for within our model. One of them is the estimate of the capacitance. We have used a simple parallel plate capacitance model for the calculation of the capacitance between the graphene flake and the substrate; this is a very good approximation in the neighborhood of $V_g^{DC} = 0$ V. However, at higher gate voltages, the electrostatic attraction causes the graphene flake to flex down (this can be of the order of ~ 10 nm) and comes closer to the substrate, which can lead to change in capacitance and its derivative. Second contribution can arise from the fact that we have used the room temperature value of the Young's modulus (1 TPa) for describing the low temperature data as well, a change in the Young's modulus can also affect the resonance frequency dispersion with gate voltage. Theoretical calculation do suggest that the assumption of constant Young's modulus over this temperature range is reasonable [1]. Thirdly, the thermal response of impurities on the flake cannot be ignored while explaining the low temperature data. And, this residue on the the flake can modify the strain estimation $\left(\frac{L-L_0}{L_0} \right)$ at low temperatures as the system acts like a composite polymer-graphene system. We have tried to captured all of these effects in the form of a parameter λ as an independent measurement is not possible from the current experiment. Further detailed measurements are required to understand the microscopic mechanisms that will be critical for strain engineering.

6. Calculation of the coefficient of thermal expansion of graphene (CTE)

As described above, the frequency dispersion with gate voltage allows us to estimate $\Gamma_0(T)$ and ρ of the graphene flake independently. And with one fitting parameter (λ), we

can completely describe the frequency dispersion with gate voltage at all temperatures. However, the resonance frequency at zero gate voltage ($f_0(0)$) solely depends on the $\Gamma_0(T)$ (see Equation 11). Therefore, using ρ calculated from the room temperature frequency-dispersion curve, we can estimate the $\Gamma_0(T)$ and hence net strain at any given temperature. Now, we consider the various contributions to the net strain in the flake. As we reduce the temperature of the device, the gold electrodes start to contract and hence increase the strain in the flake. Next is the contribution from substrate. Different coefficients of thermal expansion of Si and SiO₂ also contribute to the net strain in the flake. At any temperature, substrate's contribution to the net strain between the electrode can be calculated using generalized Stoney's formula [2] and is given by,

$$\epsilon_{substrate}(T) = -\frac{d_{SiO_2}E_{SiO_2}(1-\nu_{Si})}{d_{Si}E_{Si}(1-\nu_{SiO_2})} \left(\int_T^{300} \alpha_{Si}(t) - \alpha_{SiO_2}(t) dt \right), \quad (12)$$

where E_{Si} and E_{SiO_2} are the Young's moduli, d_{Si} and d_{SiO_2} are the thicknesses, ν_{Si} and ν_{SiO_2} are the Poisson's ratio, and $\alpha_{Si}(T)$ [3] and $\alpha_{SiO_2}(T)$ [4] are the coefficient of thermal expansion of silicon and silicon oxide respectively. We can now write an effective coefficient of thermal expansion for trench as $\alpha_{trench} = \frac{d\epsilon_{substrate}(T)}{dT}$. The value α_{trench} at room temperature can be estimated by taking, $d_{SiO_2} = 300\text{nm}$, $d_{Si} = 300\mu\text{m}$, $E_{Si} = 160\text{GPa}$, $E_{SiO_2} = 70\text{GPa}$, $\nu_{Si} = 0.22$, $\nu_{SiO_2} = 0.16$. By using the thermal expansion coefficient for Si and SiO₂ as a function of temperature [3, 4], we estimate, $\alpha_{trench}(300) = -8.1 \times 10^{-10} K^{-1}$ and $\alpha_{trench}(30) = -2.0 \times 10^{-10} K^{-1}$. Therefore, substrate's contribution to the net strain in the flake can be neglected. Third, the expansion/contraction of the graphene flake itself changes the net in-built tension in the flake. By combining all these contributions to strain at any given temperature, we can write the net built-in tension in the flake as,

$$\Gamma_0(T) = \Gamma_0(300) + \frac{E_{graphene}wt}{L} \left(L \int_{300}^T \alpha_{graphene}(T) dT - w_{electrode} \int_{300}^T \alpha_{gold}(T) dT \right) + E_{graphene}wt\epsilon_{substrate}(T) \quad (13)$$

Using 11 and assuming a uniform contraction/expansion of gold electrodes, we can write,

$$\alpha_{graphene} = -\frac{w_{electrode}}{L} \alpha_{gold}(T) - \frac{4L^2\rho}{E_{graphene}} 2f_0(0) \frac{df_0(0)}{dT} + \frac{d\epsilon_{substrate}(T)}{dT} \quad (14)$$

7. Variation of quality factor (Q) with temperature

On cooling the graphene electromechanical resonators the resonance frequency as well as quality factor (Q) increase. Figure 5 shows the variation of Q with temperature from device as it can be seen that Q can be increased by a factor of four this device. Similar increase in Q can also be seen in the Figure 2a in the main text, where narrowing of the resonance peak with temperature is very evident. All the devices we measured showed increase in Q upon cooling. The observation that the increase in resonant frequency is accompanied by an increase in the Q suggests that the loss mechanism

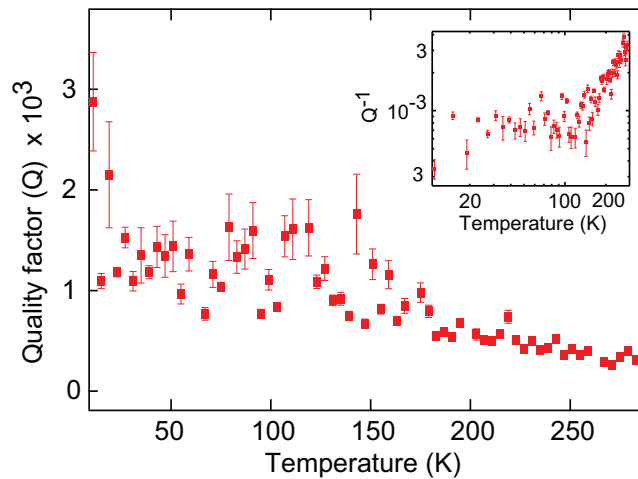


Figure 5. The plot shows the variation of the quality factor of resonance with temperature. The inset shows the plot of Q^{-1} with temperature.

may be frequency independent[5]. The inset of the figure shows the plot of Q^{-1} , which is directly proportional to the dissipation in the resonator, with temperature. At lower temperatures, dissipation reduces more slowly than compared to the temperatures greater than 100K. Similar behavior has been observed by Chen *et al.* [6]

References

- [1] Jin-Wu Jiang, Jian-Sheng Wang, and Baowen Li. Young's modulus of graphene: A molecular dynamics study. *Physical Review B (Condensed Matter and Materials Physics)*, 80(11):113405–113404, 2009.
- [2] L. B. Freund and S. Suresh, editors. *Thin Film Materials*. Cambridge University Press, 2003.
- [3] K. G. Lyon, G. L. Salinger, C. A. Swenson, and G. K. White. Linear thermal expansion measurements on silicon from 6 to 340 k. *Journal of Applied Physics*, 48(3):865–868, 1977.
- [4] G. K. White, J. A. Birch, and Murli H. Manghnani. Thermal properties of sodium silicate glasses at low temperatures. *Journal of Non-Crystalline Solids*, 23(1):99–110, 1977.
- [5] Vera Sazonova. *A tunable carbon nanotube resonator*. PhD thesis, Cornell University, 2006.
- [6] Changyao Chen, Sami Rosenblatt, Kirill I. Bolotin, William Kalb, Philip Kim, Ioannis Kymissis, Horst L. Stormer, Tony F. Heinz, and James Hone. Performance of monolayer graphene nanomechanical resonators with electrical readout. *Nat Nano*, advance online publication, 2009.